

Nanoparticles of Ti and Zr in organosilicon polymer ceramic precursors

Sergei P. Gubin,^{a*} Ella M. Moroz,^b Andrei I. Boronin,^b Vladimir V. Kriventsov,^b Dmitrii A. Zyuzin,^b Nina A. Popova,^c Elena K. Florina^c and Alexander M. Tsirlin^c

^a N. S. Kurnakov Institute of General and Inorganic Chemistry, Russian Academy of Sciences, 117907 Moscow, Russian Federation. Fax: +7 095 954 1259

^b G. K. Boreskov Institute of Catalysis, Siberian Branch of the Russian Academy of Sciences, 630090 Novosibirsk, Russian Federation. Fax: +7 383 234 3056

^c State Scientific Centre, Institute of Chemistry and Technology of Organoelement Compounds, 111123 Moscow, Russian Federation. Fax: +7 095 273 1323

A procedure was developed for introducing Ti and Zr nanoparticles into organosilicon polymer ceramic precursors; all of the particles were found to be multiphase and to contain the metals, metal carbides, and metal oxides associated with the polymer matrix.

Organic polymers that contain metal nanoparticles occupy a significant place among nanostructured materials, the interest in which is currently growing like an avalanche.¹ Metal nanoparticles ($d < 10$ nm) are unstable and highly reactive; they attracted considerable interest because of their unique physical properties. The up-to-date level of ceramic polymer technology is sufficiently high, and therefore, polymer matrices are preferable for the stabilisation of metal nanoparticles from the practical standpoint of the material science.

It is well known that refractory metal heteroatoms of (Ti, Zr *etc.*) are effective stabilisers for ultrafine ceramic structures. Moreover, they also give an improvement in the refractory properties, thermal resistance and sintering ability.² The direct introduction of metals into a ceramics is a rather difficult task because homogeneous distribution of metal nanoparticles in the solid structure is required, and no additional oxygen should be introduced. It is believed that the formation of ceramic materials *via* polymeric precursors³ opens up a new and effective way in this direction on condition that new methods for introducing metal nanoparticles will be developed.

In recent years the problem of polymer stabilisation by metal nanoparticles has provoked considerable interest. Some ways have been proposed to introduce metal nanoparticles into organic polymer matrices. In chemically inert linear polymers such as polyethylene, metal nanoparticles are usually formed *in situ* as a result of fast thermal decomposition of a solution of metal-containing compounds, which is introduced into a polymer solution or melt.⁴ The metal nanoparticles (stabilisers) primarily react with oxygen to yield inert products and hence prolong the lifetime of the polymer (prevent the degradation).⁵

In this study, polycarbosilane was chosen as the basic polymer; this ceramic precursor is usually formed by thermal rearrangement of polydimethylsilane.⁶ Polycarbosilane is a low-molecular-weight polymer ($MM = 1200\text{--}2000$) with active Si-H and Si-C bonds; it is considerably different from polyethylene as a matrix. We performed a detailed investigation of the polydimethylsilane conversion into polycarbosilane to find optimum time and temperature for the introduction of metal-containing compounds. The intermediate and final products of polymer transformations were analysed by NMR, UV and IR spectroscopy, gas chromatography-mass spectrometry, gas chromatography and high-performance liquid chromatography.

For the formation of Ti- and Zr-containing metal nanoparticles, we decided on oxygen-free compounds of these metals. We found that thermal decomposition of MCl_4 ($M = \text{Ti}$ or Zr) requires a large amount of active Si-H hydrogen to reduce the metal during the formation of metal nanoparticles. A different situation arises with thermal decomposition of $(C_6H_5CH_2)_4Ti$ in polycarbosilane: toluene and dibenzyl (1:3) were quantitatively detected in the distillation products. That is, all benzyl radicals from the initial metal-containing compound⁷ predominantly undergo a homotransformation to release naked hot metal atoms, which become aggregated into metal nano-

particles. Cp_2MCl_2 ($M = \text{Ti}$ or Zr) exhibits an intermediate behaviour under conditions of thermal degradation. It was experimentally found that the principal features of the process are the same as in the case of polyethylene: drop-by-drop addition and very fast thermal decomposition of metal-containing compounds, complete removal of organic ligands and homogeneous distribution of metal nanoparticles as a result of intense agitation of the oligomer/polymer reaction mixture.

It is believed that the polymer melt contains a large number of cavities (domains) distributed throughout a continuous medium. The decomposition of metal-containing compounds and subsequent particle nucleation proceed in these cavities.⁸ The transformation of polydimethylsilane into polycarbosilane at $300\text{--}380^\circ\text{C}$ usually takes about 28 h. It was found that the introduction of metals at an intermediate stage of synthesis is most effective. If the reaction is carried out in the presence of the products of thermal decomposition of the above Ti- or Zr-containing compounds, the reaction time can be shortened to 3–5 h. The process speeds up after the introduction of metals; however, any negative side effects were not detected. The study showed that, in this case, metal nanoparticles took part in rearrangement and polycondensation. An optimum time of contact between metal nanoparticles and the reaction mixture depends on the number of Si-Si bonds to be ruptured. The presence of additional Si-H groups in the polymer provides an opportunity to graft new active functional groups. The aforesaid suggests more active interaction between metal nanoparticles and polycarbosilane as compared with carbon-chain polymers.

Polycarbosilane samples containing metal nanoparticles (nano-MPCS) with the Ti or Zr content no higher than 5 wt% were prepared from different metal-containing compounds.[†] Two

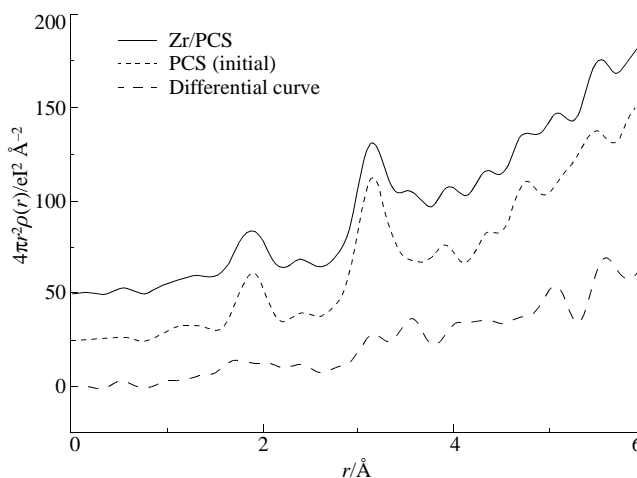


Figure 1 X-ray RED curves for nano-ZrPCS.

[†] Satisfactory analyses for C, H, Si and metals were obtained for all samples by standard procedures.

series of analytical experiments were carried out with these materials. First of all, the polymeric portion of nano-MPCS was examined in comparison with the initial metal-free polycarbosilane. It was found that the method used for preparing nano-MPCS did not introduce additional oxygen, provided more regular polymeric structure and increased the amount of Si-H groups. The molecular-weight distribution (MWD) is consistent with that of the best samples of starting polycarbosilane. A narrow unimodal MWD a polydispersity index of about 2 was observed. The average molecular weight lied in the range 1000 to 1200. High-molecular-weight components (tails) were absent.[‡] According to their rheological characteristics, nano-MPCS can be used as spinning melts at lower temperatures in comparison with unmodified polycarbosilane. A viscosity[§] of about 1000 P, which is needed for the spinnability, was achieved at about 120–150 °C instead of initial 250–280 °C. Preliminary experiments showed that metal contents of up to 3% did not prevent stable spinning of fibres.

TGA[¶] of nano-ZrPCS exhibited a considerably larger yield of the solid phase (up to 10% at 1.0–1.3% of the metal) in comparison with the initial polycarbosilane. DSC analysis showed active exothermic processes over a broad temperature range and demonstrates some differences between nano-TiPCS and nano-ZrPCS. The behaviour of the latter is similar to that of the starting polycarbosilane. This is likely due to the well-known fact that titanium, especially finely divided, exhibit higher catalytic activity.

The nature of metal nanoparticles in polycarbosilane matrices was also analysed. Earlier, we have examined similarly obtained samples of model nano-MPCS containing up to 5 wt% Fe using X-ray emission and Mössbauer spectroscopy.⁹ We have found that polycarbosilane as a matrix does not differ from other examined polymers in both the structure of nanoparticles and the particle-size distribution: more than 80% of particles had a size of no more than 5 nm. All particles were multiphase: they contained iron, iron carbide and iron oxides. The formation of a FeSi phase was reliably detected; bonds between nanoparticles and the matrix were also detected as in other nanometallic polymers.¹⁰ It is known that Ti and Zr nanoparticles exhibit the highest chemical activity; thus, it is clear that their effect on transformations of the matrix will be no less than that of Fe nanoparticles.

The phase analysis of nano-MPCS samples (M = Ti or Zr) was performed by two techniques. One of them consisted in the construction of radial electron-density distribution functions obtained from the intensity curve of X-ray scattering (X-ray RED), and the other was EXAFS spectroscopy. The advantage of EXAFS spectroscopy consists in its selectivity, which makes it possible to obtain the atomic radial distribution curve for the local arrangement of a selected chemical element in the sample. Both of these techniques give interatomic distances (r) and coordination numbers (Z), which can be compared with those calculated from structural data for a particular phase. Thus, X-ray RED and EXAFS techniques inspect and supplement each other.

Experimental EXAFS data^{††} on r and Z for nano-ZrPCS showed that the sample contained zirconium metal (the interatomic distances 3.11, 3.27 and 5.58 Å agree well with the calculated data). The peak with $r = 1.97$ Å can be assigned to the Zr–C distance and is indicative of the metal–matrix interaction. The ZrO₂ phase was absent from the sample since there are no Zr–Zr and Zr–O peaks characteristic of this phase. The alternative results were obtained by EXAFS for nano-TiPCS: the sample contained both the metal phase and the

TiO₂ phase (probably anatase). The distance $r = 1.82$ Å may correspond to the Ti–C bond resulting from partial replacement of silicon in the Si–C chains of a polymeric matrix.

X-ray diffraction analysis showed that all samples were amorphous; this means that the size of the crystallites (nanoparticles) is less than 20 Å. Figure 1 compares the RED curve of nano-ZrPCS with the RED curve of the initial matrix;^{‡‡} a differential curve is also presented. As in the case of EXAFS, the differential curve exhibits peaks due to the Zr⁰ phase ($r = 3.20$ and 5.60 Å). The phase composition of metal nanoparticles in the nano-TiPCS sample is different: both metal and oxide phases were observed. The modelling of X-ray RED curves showed that the inserted Ti is distributed between the Ti⁰ and TiO₂ phases in the ratio 1:5 (Figure 2). The formation of TiO₂ in the nano-TiPCS sample was supported by XPS analysis.^{§§} The spectrum of Ti 2p_{3/2} consists of three components; for chemical identification, we need to discuss only the peaks with $E_b = 455.0$ and 459.2 eV. According to reference data,^{14,15} the peak with $E_b = 459.2$ eV can be reliably assigned to Ti–O bonds in titania or titanate. The component with $E_b = 455.0$ eV may be attributed to the Ti–C bond. Note that bulk metallic Ti has $E_b = 454.0$ eV, but the corresponding value for Ti nanoparticles is unknown for us.

Note that modifications of matrices in the course of the formation of metal-containing polycarbosilane can be observed in the differential RED curve: there is strong disordering of bonds with lengths of about 2 and 4–5 Å in the case of nano-TiPCS. Analogous changes were observed for the nano-ZrPCS sample; it is not improbable that they are associated with the introduction of nanoparticles deep within the polymer structure. The XPS analysis also showed that no Ti or Zr (to within the limit of detection of 0.1–1 at%) were present at the surface of the investigated samples. Using long scanning it was possible to record the Ti 2p line and to determine the Ti concentration near the surface film to be equal to 2×10^{-2} at%; this value is lower

^{††}The EXAFS spectra of K-edges of Ti or Zr were obtained on the EXAFS spectrometer at the Siberian Synchrotron Radiation Centre. The VEPP-3 storage ring with an electron-beam energy of 2 GeV and an average stored current of 80 mA were used as the radiation source. The X-ray energy was monitored with a channel cut Si(111) monochromator. All of the spectra were recorded in the transmission mode using two ionisation chambers as detectors. The harmonics rejection was performed for the Ti K-spectra. For the EXAFS measurements, the samples were prepared as pellets with thickness varied so that a 0.5–0.8 jump at the absorption K-edges of Ti or Zr was obtained. The EXAFS spectra were treated using standard procedures.¹¹ The background was removed by extrapolating the pre-edge region to the EXAFS region in the form of Victoreen's polynomials. Three cubic splines were used to construct the smooth part of the absorption coefficient. The inflection point of the edge of the X-ray absorption spectrum was used as the initial point ($k = 0$) of the EXAFS spectrum. The radial distribution of the atoms (RDA) function was calculated from the EXAFS spectra as $k^3\chi(k)$ using the Fourier analysis for the wavenumber range $k = 4.0$ – 12.0 Å^{−1}. A curve fitting procedure with the EXCURV92 program¹² was employed to determine precisely the distances, coordination numbers and the Debye–Waller factors. This was performed for $k^3\chi(k)$ over a similar wavenumber range after preliminary Fourier filtering with engaging known XRD data for bulk compounds.

^{‡‡}X-ray RED: diffractometer; CuK α radiation monochromated with a graphite monochromator; all samples were X-ray amorphous; the diffraction pattern of the matrix had a wide halo with the intensity maximum at the interplanar distances $d/n = 8.8$ Å; this halo is shifted to $d/n = 8.4$ Å upon introducing Ti or Zr. For calculating the RED curves for all of the samples, the intensities of X-ray scattering in the angle range 3 to 150° (2θ) at MoK α radiation were measured. For determining the phase composition of the supported component and the modification of a polymeric matrix (polycarbosilane), the difference RED curves were constructed; the technique for calculating the RED curves was described in ref. 13.

^{§§}The samples were analysed on a VG ESCALAB HP electron spectrometer. The samples were applied to a rough surface of copper plates or to the surface of an adhesive tape by pressing and powdering. Survey scans with the high pass energy $HV = 100$ eV were recorded to obtain high-sensitivity spectra. Particular spectral lines were taken with high resolution using $HV = 20$ eV.

[‡] MWD curves were obtained by exclusive gel-permeation chromatography on Shodex styrogel columns (Knauer) with a UV detector. Dry THF was used as a solvent, and polystyrene was used as the reference substance for calibration.

[§] Rheological characteristics were measured in an argon atmosphere using a Reotest-Lovo instrument; the heating rate was 5–10 K min^{−1}.

[¶] TGA was performed within the range 20–800 °C (He, 5 K min^{−1}); DSC analysis was performed at 20–600 °C in Ar; 2, 5 or 10 K min^{−1} (DuPont).

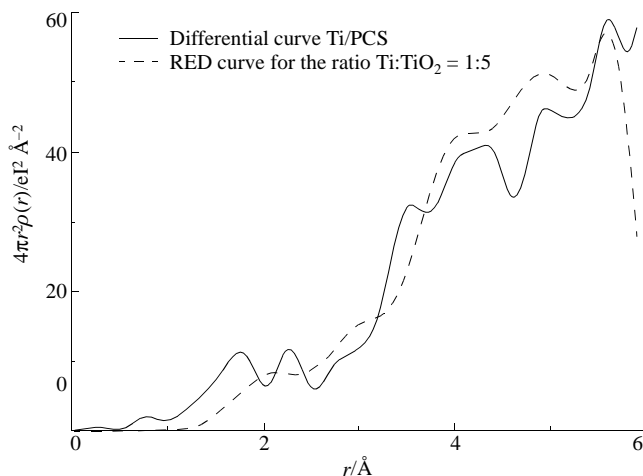


Figure 2 Modelling of differential X-ray RED curves for nano-TiPCS.

than the Ti concentration in the sample. This observation can be easily explained by an effect of capsulation of Ti nanoparticles inside the cavities (domains) of an organic polymer matrix.

This work was supported by INTAS (grant no. 96-1410) and by the Russian Foundation for Basic Research (grant no. 98-03-32677).

References

- 1 (a) K. E. Drexler, *Nanosystems: Molecular Machinery, Manufacturing, and Computation*, New York, Wiley, 1992; see also (b) S. L. Gillett, *Nanotechnology*, 1996, **7**, 168.
- 2 C. Y. Ho and S. K. El-Rahaiby, *Ceram. Eng. Sci. Proc.*, 1992, **13**, 3.

- 3 A. M. Tsirlin, V. G. Gerlivanov, N. A. Popova, S. P. Gubin, E. K. Florina, B. I. Shemaev and E. B. Reutskaya, *ECCM-8, Symposium 6*, Naples, 1998, **4**, 137.
- 4 S. P. Gubin and I. D. Kosobudskii, *Usp. Khim.*, 1983, **52**, 1350 (*Russ. Chem. Rev.*, 1983, **52**, 766).
- 5 E. B. Brun, O. A. Shustova, S. I. Kuchanov and G. P. Gladyshev, *J. Polymer Sci.*, 1980, **18**, 2461.
- 6 T. Ishikawa, M. Shibuya and T. Yamamura, *J. Mater. Sci.*, 1990, **25**, 2809.
- 7 U. Zucchini, E. Albizzati and U. Giannini, *J. Organomet. Chem.*, 1971, **26**, 357.
- 8 T. W. Smith and D. Wychick, *J. Phys. Chem.*, 1980, **84**, 1621.
- 9 S. P. Gubin, A. V. Kozinkin, M. I. Afanasov, N. A. Popova, O. V. Sever, A. T. Shuvaev and A. M. Tsirlin, *Neorg. Mater.*, 1999, **35**, 237 (in Russian).
- 10 A. V. Kozinkin, V. G. Vlasenko, S. P. Gubin, A. T. Shuvaev and I. A. Dubovtsev, *Neorg. Mater.*, 1996, **32**, 422 [*Inorg. Mater. (Engl. Transl.)*, 1996, **32**, 376].
- 11 D. J. Kochubey, *EXAFS spektroskopiya katalizatorov (EXAFS spectroscopy of catalysts)*, Nauka, Novosibirsk, 1992 (in Russian).
- 12 N. Binsted, J. V. Campbell, S. J. Gurman and P. C. Stephenson, *SERC Daresbury Laboratory EXCURVE-92 Program*, 1991.
- 13 E. M. Moroz, *Usp. Khim.*, 1992, **61**, 188 (*Russ. Chem. Rev.*, 1992, **61**, 356).
- 14 *Handbook of X-ray Photoelectron Spectroscopy*, ed. G. E. Muilenberg, Eden Prairie, Minnesota, 1978, p. 190.
- 15 *Handbook of X-ray Photoelectron Spectroscopy*, ed. J. Chastain, Eden Prairie, Minnesota, 1992, p. 261.

Received: Moscow, 1st September 1998

Cambridge, 17th November 1998; Com. 8/07872F